The effects of the E3 ubiquitin–protein ligase UBR7 of Frankliniella occidentalis on the ability of insects to acquire and transmit TSWV

Jun-Xia Shi
China Agricultural University
Jun-Xian Zhou
Agricultural Technology Service Center of Yunyang County
Fan Jiang
Chinese Academy of Inspection and Quarantine
Zhi-Hong Li
China Agricultural University
Shuifang Zhu (zhusf@caiq.org.cn)
China Agricultural University

Research Article

Keywords: Frankliniella occidentalis, Tomato spotted wilt orthotospovirus, E3 ubiquitin–protein ligase, UBR7, Transmission efficiency

Posted Date: June 16th, 2022

DOI: https://doi.org/10.21203/rs.3.rs-1755807/v1

Abstract

The interactions between plant viruses and vector insects are complex. In recent years, RNA Sequencing data have been used to elucidate the key genes of *tomato spotted wilt orthotospovirus* (TSWV) and *Frankliniella occidentalis* (*F. occidentalis*). However, very little is known about the key genes involved in thrip acquisition and transmission of TSWV. On the basis of the transcriptome data of *F. occidentalis* with TSWV, we verified the complete sequence of the E3 ubiquitin-protein ligase *UBR7* gene (*UBR7*), which was closely related to virus transmission. Additionally, we found that UBR7 belongs to the E3 ubiquitin–protein ligase family, which was highly expressed in adulthood of *F. occidentalis*. The transmission efficiency of *F. occidentalis* decreased with low *URB7* expression, while the acquisition efficiency was not affected. Moreover, the direct interaction between UBR7 and the nucleocapsid (N) protein of TSWV was investigated through surface plasmon resonance and GST pull-down. In conclusion, we found that UBR7 is a key protein for TSWV transmission of *F. occidentalis*, which directly interacts with TSWV N. This study provides a new direction for the development of green pesticides targeting E3 ubiquitin to control TSWV and *F. occidentalis*.

Introduction

Tomato spotted wilt orthotospovirus (TSWV), a member of the order *Bunyavirales*, family *Tospoviridae* and genus *Orthotospovirus*, was first discovered by Brittlebank in Australia in 1915 (Bewley, 1922; Brown, 1930). In the last decade, due to climate change, human activities, agricultural production, and arthropod spread, the incidence of TSWV has been increasing (Liang et al. 2020; Mandal et al. 2007; Sivaprasad et al. 2018). TSWV can infect more than 1,060 plants in 85 families (Scholthof et al. 2011). Because of the significant damage, TSWV was listed as one of the world's 10 most harmful plant viruses (Scholthof et al. 2011). The European and Mediterranean Plant Protection Organization (EPPO) classifies it as an A2 quarantine pathogen.

TSWV is only spread by thrips, such as western flower thrips (*Frankliniella. occidentalis*), flower thrips (*F. intonsa*), palm thrips (*Thrips palmi*), tobacco thrips (*T. alliorum*)(Ullman et al. 2002). The western flower thrips (*F. occidentalis* (Pergande)) were the dominant species for the transmission of TSWV and have attracted much attention. Because of its small size, good concealment, agile action, rapid reproduction, broad host range, and high drug resistance, it has brought severe economic losses to many countries and regions (Gupta et al. 2018). The EPPO also classifies *F. occidentalis* as an A2 quarantine pest. And China has included *F. occidentalis* in the IAS1000 Project (A genome project of 1000 invasive alien species).

During the transmission of TSWV by *F. occidentalis*, TSWV needs to replicate and break through the mediator's multiple infection barriers to reach the salivary glands of thrips. TSWV first infects the midgut epithelial cells of *F. occidentalis* (Gupta et al. 2018). After TSWV infects thrips, it replicates in multiple organs, similar to the mode of other *Bunyavirales* virus infections (Whitfield et al. 2005). *Frankliniella occidentalis* is mainly infected by feeding on plants infected during the first instar larval stage. Furthermore, TSWV proliferates in the salivary glands and other tissues of *F. occidentalis* (Wetering et al. 1996). Infected adult insects carry the virus for life and spread it by feeding on healthy plants, thus infecting them (Wetering et al.1996). Therefore, identifying the key proteins that affect the transmission of TSWV by *F. occidentalis* is crucial to understand the relationship between pathogens and hosts. Which is also the basis for the control measures of TSWV and its transmission vector *F. occidentalis.*

However, little is known about thrips' response to TSWV during the infection process, from larval acquisition to adult inoculation of plants. RNA Sequencing (RNA-seq) is a powerful tool for identifying differentially expressed transcripts during host–pathogen interactions. Therefore, several RNA-seq based transcriptome analyses have been performed to determine the differentially expressed genes in TSWV-infected *F. occidentalis* (Schneweis et al. 2017; Shrestha et al. 2017; Zhang et al. 2013). The first study identified 278 unigenes related to insecticide resistance (Zhang et al. 2013). Schneweis used RNA-seq to determine the overall transcriptome response of first instar larvae, pupae, and adults of *F. occidentalis* to viral infection. The differentially expressed putative innate immunity-related transcript genes mainly include: zinc finger protein; hexamerin 2 B; thyroid peroxidase precursor (Schneweis et al. 2017). The gene library that responds to TSWV is different during different developmental stages, which reflects the relationship between thrip development and virus transmission in insect vectors, and indicates coordination between development and the virus dissemination route (Schneweis et al. 2017; Shrestha et al. 2017). Transcriptomic and network integration analysis of the larval gut of *F. occidentalis* found that zinc finger protein was associated with TSWV (Han and Rotenberg 2021). Additionally, we have referred to the primary sequence of a draft genome of *F. occidentalis* and three developmental-stage transcriptomes to identify TSWV responsive genes (Schneweis et al. 2017). According to the inference of response gene ontology, TSWV infection interferes with host defense; insect cuticle structure; and development, metabolism, and transport processes and functions. Functional annotation of these differentially expressed genes showed that these were primarily related to host defense, insect cuticle structure, development, metabolism, and transport. Moreover, most of these studies are at the level of sequencing and prediction, and there are few basic biological studies on the interaction between TSWV and *F. occidentalis*. Wan successfully constructed a yeast two-hybrid library and TSWV membrane protein G_N and G_C bait vector in 2019 (Wan et al. 2019) and subsequently screened proteins interacting with TSWV G_N in 2020, including ubiquitin-related proteins (Zheng et al. 2020). The interaction between TSWV and the ubiquitin–protein of *F. occidentalis* was demonstrated again at the protein level.

Ubiquitin, one of the most common posttranslational protein modifiers, is widely and highly conserved in all eukaryotes. The ubiquitination process, consisting of a tertiary enzyme-linked reaction consisting of an E1 ubiquitin-activating enzyme, E2 ubiquitin-conjugating enzyme, and an E3 ubiquitin–protein ligase, is an important posttranslational modification (PTM) and protein degradation process and an important method of protein interaction between host and pathogen (Alejandro et al. 2019; Schinz and Littlefield 1985). Viruses use host cells to synthesize proteins that influence and control the host, so protein expression in the host is conducive to viral proliferation (Snippe et al. 2005). The E3 ubiquitin–protein ligase system in the host can selectively degrade viral proteins, limiting the growth of the virus so that both virus and host reach and form a steady state (Tang et al. 2018). To counter the antiviral mechanism of the host ubiquitin–proteasome system (UPS), UPS is the main target of the virus, which evolves to use or destroy UPS to inactivate or degrade cellular proteins to promote viral reproduction (Tang et al. 2018). UBR7 protein of E3 ubiquitin–protein ligase family, encodes a UBR box-containing protein (zinc finger in n-recognin) and contains a plant homeodomain (PHD) in the C-terminus (Dasgupta et al. 2022). And UBR7 plays a role in the N-terminal rule proteolytic pathway, which is function highly conserved in yeast, animals, and plants (Lee et al. 2008; Zimmerman et al. 2014). A study based on TurboID used proximity

labeling to prove that the UBR7 protein in the E3 ubiquitin–protein ligase family directly interacts with the nucleocapsid (N) protein of *Tobacco mosaic virus* (TMV) and that UBR7 is an immune regulator mediated by plant nucleotide-binding leucine-rich repeat immune receptors (Lee et al. 2008; Zimmerman et al. 2014). However, its function is still not well understood and there is no research in thrips.

Here, we verified the *UBR7* gene, a protein closely related to TSWV, from *F. occidentalis* using existed data (Schneweis et al., 2017). And we detected the expression of the *UBR7* gene in different *F. occidentalis* instars, and explored the effect of UBR7 in acquisition and transmission of TSWV. Surface plasmon resonance (SPR) and GST pull-down assays were used to demonstrate the direct interaction between the UBR7 protein of *F. occidentalis* and the TSWV N protein. The aim was to provide insights for the research and development of novel molecular drugs for the simultaneous targeted control of TSWV and thrips.

Materials And Methods

1. Plant materials and TSWV inoculum

Datura stramonium plants were kept in a growth chamber at 25°C with a 16-h light/8-h dark photoperiod.

TSWV was a gift from the Nanjing Agricultural University. This virus was maintained on *Datura stramonium* plants (Wan et al. 2018). TWSV-infected plant tissue for the acquisition access period (AAP) was obtained by mechanical inoculation of 3-week-old *D. stramonium* plants or through *F. occidentalis* insect vectors (Zhao et al. 2016). Infected tissue was ground in a chilled mortar and pestle in 10 mL of general extract buffer (Agdia, Indiana, USA). Plants to be inoculated were dusted with carborundum and gently rubbed with a cotton swab wetted with inoculum. Twelve days after mechanical inoculation, the leaves appeared deformed, curled, chlorotic, stained and other symptoms.

2. Insect culture

Frankliniella occidentalis, a susceptible laboratory strain, was a gift from the Institute of Vegetables and Flowers, Chinese Academy of Agricultural Sciences. The *F. occidentalis* colony was maintained on green beans (*Phaseolus vulgaris*) at 25°C, 50% relative humidity, and an L16:D8 photoperiod (Montero-Astúa, Ullman, and Whitfield, 2016).

Fresh beans were placed in the insect cage for the adult thrips to lay eggs. After 3 days, the thrips were removed with a brush, and the beans were placed in a new cage. The larvae were allowed to incubate and were fed with *D. stramonium* with or without TSWV for 72 h and then fed with green beans until they emerged as adults. First instar larvae (L1s), second instar larvae (L2s), pupae, female adults, and male adults of thrips were collected according to the methods of previous studies (Akoth, Pascal, Hans-Michael, and Pappu, 2016; Zhi, LI, and Gai, 2010). Subsequently, different developmental stages were collected for total RNA extraction. The experiments were repeated six times for each developmental stage ($n \geq 6$).

3. Cloning of the *UBR7* gene

3.1. RNA isolation and first-strand cDNA synthesis

Total RNA of adult *F. occidentalis* with TSWV was extracted using TransZol Up Reagent (TransGen, Beijing, China). Then, RNA integrity was further affirmed using agarose gel electrophoresis. Genomic DNA elimination and reverse transcription was conducted using TransScript® II One-Step gDNA Removal and cDNA Synthesis SuperMix kit (TransGen, Beijing, China). The synthesized cDNA was stored at −20°C for further use.

3.2. Cloning of the full-length *UBR7* cDNAs

On the basis of the National Center for Biotechnology Information (NCBI) data (Schneweis, Whitfield, and Rotenberg, 2017), primer sequences were designed using Primer Premier 5.0 software to verify the full-length *UBR7* gene (Table. 1). Then, according to the 2 × TransTaq® High Fidelity PCR SuperMix I (-dye) kit (TransGen, Beijing, China), PCR amplification was conducted in an Applied Biosystems Veriti™ Dx 96-Well Fast Thermal Cycler (Thermo, Massachusetts, USA). Then purified PCR products were ligated into the pClone007 Vector (Tsingke, Beijing, China) and were transformed into Trans5α Chemically Competent Cell (TransGen, Beijing, China). Positive clones were selected by ampicillin resistance and then sequenced by Tsingke Biotechnology in Beijing, China.

3.3. Gene characterization and phylogenetic analysis

UBR7 gene sequence analysis was performed using the NCBI Basic Local Alignment Search Tool (BLAST) program. ScanProsite was used to speculate functional sites. The molecular weight and isoelectric point of the deduced protein sequences were computed using the ExPASy Proteomics Server. The physicochemical properties of UBR7 were evaluated through Protparam. To analyze the sequence homology and phylogenetic relationships of *UBR7*, E3 ubiquitin-protein ligase gene information from different species (including *Thrips palmi*, *Cryptotermes secundus*, *Pediculus humanus corporis*, *Nilaparvata lugens*, and *Laodelphax striatellus*) was downloaded from GenBank. Then, a phylogenetic tree was constructed using the neighbor-joining method with 1,000 bootstrap replicates through MEGA5 (Nei et al. 2013).

The amino acid sequences (AAs) were downloaded from NCBI GenBank (including *Solanum*, *Nicotiana*, *Datura*) for the multiple sequence alignment. To visualize the conserved motifs, the AAs were analyzed with Clustal and T-coffee. WebLogo illustrated the amino acid frequencies.

4. *UBR7* gene interference

4.1. dsRNA synthesis

Primers for RNA interference (RNAi) was designed using Harvard's SnapDragon program based on UBR7 gene sequence. The T7 promoter sequence (-TAATACGACTCACTATAGGG-) was added to the 5' of the forward and reverse primers. After pretest screening, we selected the dsRNA primer with the highest interference efficiency (Table. 1).

The PCR was then carried out using ds-UBR7 primers and the negative control EGFP (ds-EGFP) primers by referring to previous studies (Table. 1) (Xiang, Li, Guo, Jiang, and Huang, 2011). The T7 RiboMAX^{TM} Express RNAi System (Promega, Wisconsin, USA) was used to synthesize dsRNA. After being measured the concentration, the samples were stored at −80°C.

4.2. dsRNA feed preparation

Sucrose was weighed and dissolved in DEPC water to prepare a solution with 30% mass fraction as feed. Then, the sucrose solution was used to dilute the dsRNA to the concentration of 500 ng/μL. There groups of feeds were subsequently prepared (blank control, CK: 30% sucrose + ddH_2O; negative control group, ds-EGFP: 30% sucrose + dsRNA-*EGFP*, and experimental group, ds-UBR7: 30% sucrose + dsRNA-*UBR7*).

4.3. Interference efficiency and survival rate detection

Fifty adult thrips without TSWV were randomly selected regardless of gender. These thrips were placed into a separate plastic cup. They were fed after incubated for a 4 hour-starvation. After 24 h, the *UBR7* expression level and the survival rate of were determined.

5. Experiments of TSWV acquiring

Collected trips in L1s were divided into three groups (CK, ds-EGFP, and ds-UBR7) and were fed an artificial diet for an AAP of 24 h. After AAP, thrips were transferred into cups, and were fed with *D. stramonium* plants carrying TSWV. After 48 h, the leaves were replaced with healthy beans, until the thrips reached to L2s. The TSWV abundance of L2 thrips was detected using real-time quantitative PCR (qPCR). The process workflow was shown in Figure 1(a).

6. Experiments of TSWV transmitting

Collected adult thrips with TSWV 3 days after eclosion and were divided into three groups (CK, ds-EGFP, and ds-UBR7), which were fed an artificial diet for an AAP of 24 h. After the AAP, the artificial diet was removed from the tube and replaced with the true leaf of a healthy *D. stramonium*, a small disc with a diameter of 5 mm. After 48 h, small disks were removed and placed in a 48-well plate, 1 mL ddH_2O was added to each well, and the plates were placed in an illumination incubator for 72 h. A double-antibody sandwich enzyme-linked immunoassay method then was used to detect the TSWV infection rate of the leaves. The process workflow was shown in Figure 1(b).

7. Real-time qPCR

The expression levels *UBR7* were examined using qPCR. Primer sequences were designed using Primer Premier 5.0 software or a reference research report (Table. 1) (Piao, Yao, He, and Fan, 2008; Qingjun et al. 2014). Then, according to the 2 × T5 Fast qPCR Mix (SYBR Green I) kit (Tsingke, Beijing, China), qPCR amplification (n = 6) was conducted in PCR system using a 20 μL reaction volume containing 10 μL 2 × T5 Fast qPCR Mix (SYBR Green I), 0.8 μL of primers (10 μM) and ~50 ng of cDNA. The reaction conditions were as follows: initial denaturation (1 min at 95°C) followed by 45 amplification cycles of 95°C for 10 s and 58°C for 60 s, and the fluorescence signal value was obtained at 60°C for 1 min. Melt curves were generated to confirm that only one specific PCR product was amplified and detected. The relative gene expression levels were calculated using $2^{-\Delta\Delta CT}$. *Actin* was used as the reference gene.

8. Western blot analysis

Total protein was extracted from thrips at different developmental stages with a sodium dodecyl sulfate sample buffer and applied for western blotting using anti-β-actin (TransGen, Beijing, China) and anti-UBR7 antibodies (AtaGenix, Hubei, China). Anti-UBR7 was prepared by predicting the antigenic determinant through BepiPred-2.0, synthesizing the peptide (Peptide 1: CKRPYPDPEDTSDDE; Peptide 2: Cys+NTPGSSSQKSNIETP), and then preparing the antibody. The antibody-reactive bands were revealed using enhanced chemiluminescence (Beyotime, Shanghai, China) and detected using photographic film. The intensity of the bands was quantified using Quantity One.

9. Enzyme-linked immunosorbent assay

Then, 100 μL of PBS was used to grind and break the small disk in method 5 Experiments of TSWV acquiring. The samples were centrifuged at 10,000 × g for 5 min, and the supernatant was transferred to a new tube for TSWV Enzyme-linked immunosorbent assay (ELISA) (Mmbio, Jiangsu, China). The positive

judgment criterion was that the absorbance values were greater than or equal to twice the negative control value (judgment criteria: positive value ≥ 2 × negative control value).

10. Surface plasmon resonance technology analysis

According to the bioinformatics analysis of UBR7, we know that it has two domains, zinc finger domain 51–115 AAs and PHD-SF superfamily 142–193 AAs, and 51–193 AAs was selected as the target fragment for expression. Using the full-length cloned plasmid as a template, the target fragment was subcloned into the pET28b+ vector. *Escherichia. coli* (*E. coli*) expressed the target protein, and a 6 × His tag was added to the N-terminal for expression and purification. The purified UBR7-domain protein and *Nicotiana benthamiana* (*N. benthamiana*) with TSWV were sent to AtaGenix for the SPR test. The protein eluate was analyzed with a LC-MS/MS, QE by BGI Genomics.

11. GST pull-down assay

The target fragment was subcloned into the pGEX-6P-1 vector using the full-length cloning plasmid of the TSWV N gene as a template. The target protein was expressed by *E. coli*, and the N-terminal GST tag was added for expression and purification.

The purified TSWV N-GST and GST proteins interacted with the UBR7 domino-His protein through BeyoMag™ Anti-GST Magnetic Beads (Beyotime, Shanghai, China). The pull-down results were analyzed using western blotting after incubation with anti-UBR7 and anti-GST (Beyotime, Shanghai, China).

12. Statistical analysis

The results were expressed as the mean ± standard error. In the following steps, all data were processed with SPSS version 19.0 (SPSS Statistics for Windows, Illinois, USA). Duncan's multiple range test followed by a one-way analysis of variance was used to compare the significant differences. Treatments not sharing a common letter were significantly different at $P < 0.05$. Alternatively, independent-sample t-tests were used to compare the differences between the two groups (*, $P < 0.05$; **, $P < 0.01$; ***, $P < 0.001$; ****, $P < 0.0001$).

Results

1. cDNA cloning and characterization

According to the transcriptome analyses by bioinformatics, the full-length cDNA sequence gene fragments were named UBR7. Protein BLAST and identity analyses of the predicted AAs of the *UBR7* gene suggested that this gene belongs to the E3 ubiquitin–protein ligase family that recognizes N-degrons and structurally related molecules for ubiquitin-dependent proteolysis or related processes through the UBR box motif. In addition to the UBR box, UBR7 also harbors a PHD finger domain (142–193 AAs), a conserved zinc finger domain (51–115 AAs). It can specifically recognize histone modifications and some DNA sequences that participate in plant life processes, including plant autoimmunity (Mouriz, López-González, Jarillo, and Piñeiro, 2015) (Figure 2).

We compared the AAs of UBR7 domain (51-193AAs) within plants readily infected by the TSWV. We found that the UBR7 AAs in this region was highly conserved (protein sequence identity NaN% = 0.56). The bigger the letter in, the more conserved the amino acid site (Figure 3). The *UBR7* gene contained an unbroken open reading frame of 1,246 nucleotides, encoding 414 amino acids. On the basis of the deduced AAs, the theoretical molecular weight of *UBR7* was predicted to 46.61 kDa with a theoretical pI of 4.89 (Table 2).

2. Phylogenetic analysis

Throughout the neighbor-joining phylogenetic tree, it was found that most of the genes related to *UBR7* were predicted to be putative E3 ubiquitin–protein ligases. The phylogenetic tree revealed that *UBR7* belongs to the E3 ubiquitin–protein ligase UBR7 *F. occidentalis* clade that was clustered with *T. palmi*, *C. secundus*, and *P. humanus corporis* in the same branch (Figure 4).

3. Expression of UBR7 in *Frankliniella occidentalis*

To investigate if the expression of the *UBR7* gene in *F. occidentalis* (V^-) is related to the developmental period, qPCR was used to detect the expression level of the *UBR7* gene in L1s, L2s, pupae, female adults, and male adults. All the different thrip instars expressed *UBR7* at the mRNA level, and the expression of *UBR7* in the adult stage was significantly different from that in the larval and pupal stages (Figure 5(a)). There was no significant difference between the L1s, L2s, and pupae stages. Meanwhile, there was no significant difference in the expression of the *UBR7* gene between female and male adults, but there were significant differences compared with other instars. This result indicated that *UBR7* may be more involved in its biological functions during the adult stage of thrips.

To determine if the protein expression level of *UBR7* corresponds with the mRNA expression level, we detected the relative expression level of UBR7 protein in thrips at different instars using western blot (Figure 5(b)). The protein expression results were consistent with the mRNA level, and the expression levels in the adult stages were significantly higher than those in other stages, with no gender difference.

4. Effects of RNAi on *F. occidentalis*

5.1. Effects of RNAi on the expression of *UBR7* gene in *F. occidentalis*

To screen for the most dominant dsRNA fragments, we synthesized five dsRNAs and tested their efficiency. After RNAi, compared with that in the CK group (blank control) and the ds-EGFP group (negative control), the *UBR7* gene in the ds-UBR7 experimental group was significantly reduced (Figure 6(a)), indicating that the *UBR7* gene in thrips (V^-) was effectively down-regulated.

5.2. Effects of RNAi on the survival rate of *F. occidentalis*

After RNAi, compared with that in the CK group and the ds-EGFP group, the survival rate of *F. occidentalis* (V^-) in the ds-UBR7 group also decreased significantly. The *UBR7* gene was mainly involved in the growth and development of *F. occidentalis* (V^-) (Figure 6(b)), and it was related to homeostatic metabolism.

5.3. Effect of RNAi on acquiring TSWV of *F. occidentalis*

To explore the effect of *UBR7* on the ability of thrips (V^-) to acquire TSWV, qPCR was used to detect the RNAi efficiency of UBR7 in thrip larvae fed on leaves with TSWV. Compared with that in the CK group and the ds-EGFP group, there was no significant difference in the ability of *F. occidentalis* in the ds-UBR7 group after RNAi. Figure 6(c) shows that *UBR7* has no effect on the ability of *F. occidentalis* to acquire TSWV. In this study, *UBR7* was only highly expressed in adult stages and was lowly expressed in the larval stage (Figure 4), indicating that it is less important in the larval stage.

5.4. Effect of RNAi on transmitting TSWV of *F. occidentalis*

UBR7 was highly expressed in the adult stage of *F. occidentalis* (Figure 4), and E3 ubiquitinase is related to the spread of the virus (Snippe et al. 2005). Therefore, we used ELISA to detect the content of TSWV in leaves to explore the effect of UBR7 on the ability of *F. occidentalis* (V^+) to transmit TSWV. After RNAi with *F. occidentalis* (V^+), the absorbance value in ds-UBR7 group was extremely significantly lower than that in CK group ($P < 0.0001$) and ds-EGFP group ($P < 0.001$) (Figure 6(d)). This result illustrated that down-regulation of the *UBR7* gene impaired the ability of thrips to transmit TSWV.

5. UBR7 protein interacts directly with TSWV N protein

The proteins interacting with UBR7-domino were screened using SPR and LC-MS/MS and then compared with the NCBI Datasets. The results showed the top five proteins with the highest scores (Table 3). And most of the matched proteins are the proteins of the virus–host *N. benthamiana* and the proteins in genus *Orthotospovirus*, such as TSWV and *Chrysanthemum stem necrosis orthotospovirus*. Among them, the highest score is the N protein of *TSWV*, which explained that UBR7 binds to TSWV N protein with high efficiency.

To further verify the results of SPR and LC-MS/MS, GST pull-down were used to verify the interaction between UBR7-domino and TSWV N again (Figure 7). Figure 7(a) shows the input, and TSWV N, GST, and UBR7 can all detect the signal, indicating that the GST pull-down system is functional. Figure 7(b) shows the pull-down result after the beads pull down. UBR7-domino could be detected after coincubation with TSWV N but not after coincubation with GST, indicating that the UBR7-domino specifically interacts directly with TSWV N protein.

Discussion

Ubiquitin is an important protein of PTM and is widely involved in the regulation of innate immune signaling pathways and which is highly conserved in all eukaryotes (Snippe et al. 2005). Ubiquitination regulates protein homeostasis, cell cycle progression, gene transcription, receptor transport, and immune response (Haglund and Dikic, 2014). While, the ubiquitination regulation is not limited in eukaryotic cells but also in virus (Gao et al. 2021; Liu et al. 2018). Many viral proteins can mimic or usurp key regulators that affect the binding of ubiquitin-like protein modifiers and ubiquitin-proteins in the host, and interfere with the corresponding enzymatic cascades to effectively promote viral replication (Gao et al. 2021; Stukalov et al. 2021). In the process of virus–host interaction, previous studies have shown that the virus has evolved strategies to exploit specific PTM processes during immune evasion (Wimmer et al. 2012).

The ubiquitination cascade process includes the sequential action of the E1 ubiquitin-activating enzyme, E2 ubiquitin-binding enzyme, and E3 ubiquitin–protein ligase (Alejandro et al. 2019; Schinz and Littlefield 1985). E3 ubiquitin–protein ligase is responsible for protein-specific ubiquitination and promotes ubiquitin transfer by producing E2 ubiquitin–protein conjugating enzyme. E3 is the key factor in the last step of the ubiquitination cascade. The high efficiency and selectivity of the ubiquitination reaction reflect the properties of E3 ubiquitin–protein ligase. Through the interaction with specific substrates, this enzyme determines spatiotemporal properties and the pathway specificity (Spratt et al. 2012). E3 ubiquitin–protein ligases are the focus of cell regulation, and is a powerful target for therapeutic intervention (Nalepa et al. 2006; Petroski, 2008). E3 ubiquitin–protein ligases are divided into three families according to the characteristic domain and the mechanism of ubiquitin transfer: the RING (including the U-box protein family), HECT (homologous to the E6AP C-terminus), and RING-in-related-RING (RBR) family (Hatakeyama and Shigetsugu 2017). Although E3 ubiquitin–protein ligases from different families can catalyze the covalent connection between ubiquitin and lysine residues in target proteins, of which the mechanisms are different (Berndsen and Wolberger 2014; Mattiroli and Sixma 2014; Zheng and Shabek 2017). RING-type E3s are the most common E3 ubiquitin–protein ligases (Deshaies and Joazeiro 2009), related to DNA

repair and immune signaling pathways (Hatakeyama and Shigetsugu 2017). UBR7 belongs to the RING-type family and encodes a UBR box-containing protein that belongs to the E3 ubiquitin–protein ligase family, with a PHD in the C-terminus (Fig. 2) (Dasgupta et al.2022). Also, plant E3 ubiquitin–protein ligase plays an important role in the regulation of hormone responses, morphogenesis, disease resistance, and abiotic stress response. Overexpression of the plant E3 ubiquitin–protein ligase BnTR1 in rapeseed and rice enhances the resistance to heat stress (Liu et al. 2013). CaRING1 silence increases the infection rate of plants to bacterial spots of red pepper (Dong et al. 2011). The UBR7 protein in the E3 ubiquitin–protein ligase family in tabacco directly interacts with the N protein of TMV (Zhang et al. 2021). The result confirmed a high similarity between *F. occidentalis* and Solanaceae plant UBR7 inferred from the alignments of deduced AAs (Fig. 3).Therefore, UBR7 is closely related to the transmission of TSWV by *F. occidentalis*.

Viruses can change the ability and behavior of thrips. Different *Orthotospovirus* strains have different degrees of influence on thrips (Gupta et al. 2018; Sarwar, 2020; Stumpf and Kennedy 2005). Viruses have indirect or direct effects on the development, reproduction, survival and feeding of thrips (Gupta, Kwon, and Kim, 2018). The volatile substances released by susceptible plants attract thrips, and the insect vectors *F. occidentalis* can accelerate the transmission of TSWV depending on the feeding mode or quantity (Shrestha et al. 2012).

In *F. occidentalis*, the high expression of the *UBR7* gene mainly occurred in the adult stage (Fig. 5), indicating the temporal specificity of UBR7. *F. occidentalis* can only transmit TSWV in adult stages when thrips acquired virus in larval stages (Wetering et al. 1996). Thus, we speculated that *UBR7* participate in the transmission of TSWV by *F. occidentalis*. The results of RNAi experiments confirmed our hypothesis, in which the down-regulation of *UBR7* attenuated TSWV transmission. Meanwhile, RNAi had little effect on the ability of thrips to acquire TWSV. The decrease of *UBR7* in larval stages indicated that it had less physiological effect in larval stages. Thrips acquire virus at L1s and L2s (Wetering et al. 1996), with a lower expression of *UBR7* in instar stages. Therefore, we concluded that the ability of thrips to acquire the virus was not significantly affected after RNAi.

In conclusion, our study found that the *UBR7* gene was involved in the process of TSWV transmission by thrips, and demonstrated the direct interaction between the *F. occidentalis* UBR7 protein and the TSWV N protein (51–199 AAs domain). UBR7 is mainly expressed and functions in the adult stage. Down-regulation of *UBR7* expression reduced the transmission efficiency of thrips. These results suggested that UBR7, as a member of the E3 ubiquitin–protein ligase family, is closely related to TSWV transmission for *F. occidentalis*.

Whether the decreased virus transmission was correlated with the UBR7 interference or the lower survival still required further validation. The molecular structure where the UBR7 protein interacts with TSWV N in *F. occidentalis* remains to be studied. Moreover, we will continue to explore whether the UBR7-targeted pesticides will help TSWV transmission and *F. occidentalis* control. Our study provides an insight on the mechanism of TSWV transmission by *F. occidentalis*.

Declarations

Ethics approval and consent to participate

Not applicable.

Consent for publication

Not applicable.

Availability of data and materials

Not applicable.

Competing interests Declarations

Conflict of interest The authors declare that they have no conflicts of interest.

Funding

This work was supported by the National Key Research and Development Program of China [2019YFC1604704].

Authors' contributions

Shuifang Zhu and Zhihong Li directed this project; Shuifang Zhu, Zhihong Li, Junxia Shi and Fan Jiang designed the study; Junxia Shi and Junxian Zhou performed the experiments; Junxia Shi analysed the data and wrote the manuscript. All authors read and approved the final manuscript.

Acknowledgements

We would like to thank the Institute of Vegetables and Flowers, Chinese Academy of Agricultural Sciences for the experimental technical guidance.

References

1. Akoth OP, Pascal M, Hans-Michael P et al (2016). Predictive Models for Tomato Spotted Wilt Virus Spread Dynamics, Considering *Frankliniella occidentalis* Specific Life Processes as Influenced by the Virus. Plos One, 11(5), e154533. 10.1371/journal.pone.0154533

2. Alejandro CC, Pedro E, Pilar AJ et al (2019). Tick-Pathogen Interactions: The Metabolic Perspective. Trends in Parasitology, 4(35), 316–328. 10.1016/j.pt.2019.01.006
3. Berndsen CE, Wolberger C (2014). New insights into ubiquitin E3 ligase mechanism. Nature Structural & Molecular Biology, 21(4), 301–307. 10.1038/nsmb.2780
4. Bewley W. (1922). Tomato diseases. Journal of the Royal Horticultural Society, 169–174
5. Brown D D. (1930). Journal of the Department of Agriculture of Victoria, Australia. Journal of the Department of Agriculture of Victoria Australia
6. Dasgupta A, Mondal P, Dalui S et al (2022). Molecular characterization of substrate-induced ubiquitin transfer by UBR7-PHD finger, a newly identified histone H2BK120 ubiquitin ligase. The FEBS journal, 289(7), 1842–1857. 10.1111/febs.16262
7. Deshaies RJ, Joazeiro C (2009). RING domain E3 ubiquitin ligases. Annual Review of Biochemistry, 78(1), 399–434. 10.1146/annurev.biochem.78.101807.093809
8. Dong HL, Choi H W, Hwang BK (2011). The Pepper E3 Ubiquitin Ligase RING1 Gene, CARING1, Is Required for Cell Death and the Salicylic Acid-Dependent Defense Response. Plant Physiology, 156(2011–2025
9. Gao P, Ma XW, Yuan M et al (2021). E3 ligase Nedd4l promotes antiviral innate immunity by catalyzing K29-linked cysteine ubiquitination of TRAF3. Nature Communications, 1194(12), 1–13. 10.1038/s41467-021-21456-1
10. Gupta R, Kwon SY, Kim ST (2018). An insight into the tomato spotted wilt virus (TSWV), tomato and thrips interaction. Plant Biotechnology Reports, 12(3), 157–163. 10.1007/s11816-018-0483-x
11. Gupta R, Kwon S, Kim ST (2018). An insight into the tomato spotted wilt virus (TSWV), tomato and thrips interaction. Plant Biotechnology Reports12), 157–163. 10.1007/s11816-018-0483-x
12. Haglund K, Dikic I (2014). Ubiquitylation and cell signaling. Embo Journal, 24(19), 3353–3359. 10.1038/sj.emboj.7600808
13. Han J, Rotenberg D (2021). Integration of transcriptomics and network analysis reveals co-expressed genes in *Frankliniella occidentalis* larval guts that respond to tomato spotted wilt virus infection. BMC Genomics, 22(1), 1–17. 10.1186/s12864-021-08100-4
14. Hatakeyama Shigetsugu (2017). TRIM Family Proteins: Roles in Autophagy, Immunity, and Carcinogenesis. Trends in Biochemical Sciences, 42(4), 297. 10.1016/j.tibs.2017.01.002
15. Heaton SM, Borg NA, Dixit VM (2016). Ubiquitin in the activation and attenuation of innate antiviral immunity. Journal of Experimental Medicine, 213(1), 1–13. 10.1084/jem.20151531
16. Lee MJ, Pal K, Tasaki T et al (2008). Synthetic heterovalent inhibitors targeting recognition E3 components of the N-end rule pathway. Proceedings of the National Academy of Sciences of the United States of America, 105(1), 100–105
17. Liang Y, Yuan CQ, Li LF (2020). First report of tomato spotted wilt virus in *Argyranthemum frutescens* in China. Journal of Plant Pathology, 102(1), 573. 10.1007/s42161-019-00463-8
18. Liu B, Cai B, Gao C (2018). Regulation of innate antiviral immunity by protein ubiquitination. Scientia Sinica (Vitae), 11(48), 10
19. Liu ZB, Wang JM, Yang FX et al (2013). A novel membrane-bound E3 ubiquitin ligase enhances the thermal resistance in plants. Plant Biotechnology Journal. 10.1111/pbi.12120
20. Mandal B, Wells ML, Martinez O et al (2007). Symptom development and distribution of Tomato spotted wilt virus in flue-cured tobacco. Annals of Applied Biology. 10.1111/j.1744-7348.2007.00153.x
21. Mattiroli F, Sixma TK (2014). Lysine-targeting specificity in ubiquitin and ubiquitin-like modification pathways. Nature Structural & Molecular Biology, 21(4), 308–316. 10.1038/nsmb.2792
22. Montero AM, Ullman DE, Whitfield AE (2016). Salivary gland morphology, tissue tropism and the progression of tospovirus infection in *Frankliniella occidentalis*. Virology, 493(39–51. 10.1016/j.virol.2016.03.003
23. Mouriz A, López GL, Jarillo JA et al (2015). PHDs govern plant development. Plant Signaling & Behavior, 7(10), e993253. 10.4161/15592324.2014.993253
24. Nalepa G, Rolfe M, Harper JW (2006). Drug discovery in the ubiquitin-proteasome system, 7(5), 596–613
25. Nei M, Peterson N, Peterson D et al (2013). MEGA5: Molecular Evolutionary Genetics Analysis Using Maximum Likelihood, Evolutionary Distance, and Maximum Parsimony Methods, 10(28), 2731–2739
26. Petroski M (2008). The ubiquitin system, disease, and drug discovery. Bmc Biochemistry, 9(Suppl 1), S7. 10.1186/1471-2091-9-S1-S7
27. Piao DH, Yao L, He YN et al (2008). Molecular cloning and sequence analysis of two types of actin cDNA from the black cutworm, *Agrotis ipsilon*. Plant Protection, 34(6), 12–19. 10.3724/SP.J.1005.2008.01043
28. Wu QJ, Zhang WW, Zhao ZJ et al (2014). Primers and Methods for Specific Detection and Absolute Quantification of Tomato Verticillium Wilt Virus.
29. Sarwar M (2020). Insects as transport devices of plant viruses. Applied Plant Virology, 381–402
30. Schinz M, Littlefield S (1985). Visions of Paradise: Themes and Variations on the GardenVisions of paradise: themes and variations on the garden.
31. Schneweis DJ, Whitfield AE, Rotenberg D (2017a). Thrips developmental stage-specific transcriptome response to tomato spotted wilt virus during the virus infection cycle in *Frankliniella occidentalis*, the primary vector. Virology, 500(226–237. 10.1016/j.virol.2016.10.009
32. Scholthof KG, Adkins S, Czosnek H et al (2011). Top 10 plant viruses in molecular plant pathology. Molecular plant pathology, 12(9), 938–954. 10.1111/j.1364-3703.2011.00752.x
33. Shrestha A, Champagne DE, Culbreath AK et al (2017). Transcriptome changes associated with Tomato spotted wilt virus infection in various life stages of its thrips vector, *Frankliniella fusca* (Hinds). Journal of General Virology, 98(8), 2156–2170. 10.1099/jgv.0.000874

34. Shrestha A, Srinivasan R, Riley DG et al (2012). Direct and indirect effects of a thrips-transmitted Tospovirus on the preference and fitness of its vector, *Frankliniella fusca*. Entomologia Experimentalis et Applicata, 145(3). 10.1111/eea.12011
35. Sivaprasad Y, Garrido P, Mendez K et al (2018). First report of tomato spotted wilt virus infecting Chrysanthemum in Ecuador. Journal of Plant Pathology, 100(1), 1. 10.1007/s42161-018-0010-5
36. Snippe M, Goldbach R, Kormelink R (2005). Tomato spotted wilt virus particle assembly and the prospects of fluorescence microscopy to study protein-protein interactions involved. Advances in Virus Research, 65(63–120. 10.1016/S0065-3527(05)65003-8
37. Spratt DE, Wu K, Kovacev J et al (2012). Selective Recruitment of an E2Ubiquitin Complex by an E3 Ubiquitin Ligase. Journal of Biological Chemistry, 287(21), 17374–17385. 10.1074/jbc.M112.353748
38. Stukalov A, Girault V, Grass V et al (2021). Multilevel proteomics reveals host perturbations by SARS-CoV-2 and SARS-CoV. Nature, 1–11. 10.1038/s41586-021-03493-4
39. Stumpf CF, Kennedy GG (2005). Effects of tomato spotted wilt virus (TSWV) isolates, host plants, and temperature on survival, size, and development time of *Frankliniella fusca*. Entomologia Experimentalis et Applicata, 114(3). 10.1111/j.1570-7458.2005.00251.x
40. Tang Q, Wu P, Chen HQ et al (2018). Pleiotropic roles of the ubiquitin-proteasome system during viral propagation. Life Sciences, S1881493696. 10.1016/j.lfs.2018.06.014
41. Ullman DE, Meideros R, Campbell LR et al (2002). Thrips as vectors of tospoviruses. Advances in Botanical Research, 36(113–140
42. Wan YR, Yuan GD, He BQ et al (2018). Foccα6, a truncated nAChR subunit, positively correlates with spinosad resistance in the western flower thrips, *Frankliniella occidentalis* (Pergande). Insect Biochemistry and Molecular Biology, 99(1–10. https://doi.org/10.1016/j.ibmb.2018.05.002
43. Wan Y, Zheng X, Yuan J et al (2019). Construction of a western flower thrip yeast two-hybrid library and TSWV membrane protein bait vectors. Chinese Journal of Applied Entomology, 1(56), 99–106
44. Wetering DV, Goldbach R, Peters D (1996). Tomato spotted wilt tospovirus ingestion by first instar larvae of *Frankliniella occidentalis* is a prerequisite for transmission. Phytopathology, 86(9), 900–905. 10.1094/Phyto-86-900
45. Whitfield AE, Ullman DE, German TL (2005). Tospovirus-Thrips Interactions. Annual Review of Phytopathology, 43(1), 459–489. 10.1146/annurev.phyto.43.040204.140017
46. Wimmer P, Schreiner S, Dobner T (2012). Human Pathogens and the Host Cell SUMOylation System. Journal of Virology, 86(2), 642–654. 10.1128/JVI.06227-11
47. Xiang H, Li MW, Guo JH et al (2011). Influence of RNAi knockdown for E-complex genes on the silkworm proleg development. Archives of Insect Biochemistry and Physiology, 76(1), 1–11. 10.1002/arch.20393
48. Zhang Y, Song G, Lal N et al (2021). Author Correction: TurboID-based proximity labeling reveals that UBR7 is a regulator of N NLR immune receptor-mediated immunity. Nature Communications, 12(1). 10.1038/s41467-021-26441-2
49. Zhang Z, Zhang P, Li W et al (2013). De novo transcriptome sequencing in *Frankliniella occidentalis* to identify genes involved in plant virus transmission and insecticide resistance. Genomics, 101(5), 296–305. 10.1016/j.ygeno.2013.02.005
50. Zhao WW, Wan YR, Xie W et al (2016). Effect of Spinosad Resistance on Transmission of Tomato Spotted Wilt Virus by the Western Flower Thrips (Thysanoptera: *Thripidae*). Journal of Economic Entomology, 109(1), 62. 10.1093/jee/tov278
51. Zheng N, Shabek N. (2017). Ubiquitin Ligases: Structure, Function, and Regulation. Annual Review of Biochemistry, 86(1), 129–157. 10.1146/annurev-biochem-060815-014922
52. Zheng XB, Wan YR, Zhang YJ et al. Identifying proteins in western flower thrips that interact with Tomato spotted wilt orthotospovirus GN. Journal of Applied Entomology, 57(03), 640–657
53. Zhi J, Li J, Gai H (2010). Life table for experimental population of *Frankliniella occidentalis* feeding on leguminous vegetables. Chinese Bulletin of Entomology, 2(47), 313–317. 10.3724/SP.J.1238.2010.00550
54. Zimmerman SW, Yi Y, Sutovsky M et al (2014). Identification and characterization of RING-finger ubiquitin ligase UBR7 in mammalian spermatozoa. Cell and tissue research, 356(1), 261–278. 10.1007/s00441-014-1808-x

Tables

Table. 1. The primer pairs for RT-PCR used in this study

Primer	Target gene	Species	Primer sequence(5' to 3')	Application	Annealing temperature (°C)
UBR7	*UBR7-F*	*Frankliniella occidentalis*	GAAAACAACCAGTCAACGAA	PCR	55
UBR7	*UBR7-R*		TAGCCACCACCATCAAAAC		
UBR7	*q-UBR7-F*	*Frankliniella occidentalis*	CAGATGATGACGAAAGTAACGC	q-PCR	55
UBR7	*q-UBR7-R*		AGCAAGGCATACACCACCTC		
Actin	*q-Actin-F*	*Frankliniella occidentalis*	GGTATCGTCCTGGACTCTGGTG	q-PCR	55
Actin	*q-Actin-R*		GGGAAGGGCGTAACCTTCA		
UBR7	*ds-UBR7-F*	*Frankliniella occidentalis*	**TAATACGACTCACTATAGGG**TGTGAACAGTGCATGAGCAA	dsRNA synthesis	58
UBR7	*ds-UBR7-R*		**TAATACGACTCACTATAGGG**GCCAAAATGTTGCTCCCTTA		
EGFP	*ds-EGFP-F*	*Aequorea victoria*	**TAATACGACTCACTATAGGG**CAGTGCTTCAGCCGCTAC	dsRNA synthesis	58
EGFP	*ds-EGFP-R*		**TAATACGACTCACTATAGGGG**TTCACCTTGATGCCGTTC		
TSWV N	*q-TSWV-F*	Tomato spotted wilt orthotospovirus	CTTGCCATAATGCTGGGAGGTAG	q-PCR	58
TSWV N	*q-TSWV-R*		TCCCGAGGTCTTTGTATTTTGC		

Table 2. Bioinformatics prediction analysis of physicochemical properties of proteins

Name	Formula	Total number of atoms	Genbank accession number	ORF (bp)	Number of amino acids	Molecular weight	Theoretical pI	Asp + Glu	Arg + Lys	Instability index	Aliphatic index	Grand average hydropa
UBR7	$C_{2007}H_{3108}N_{558}O_{662}S_{30}$	6365		1246	414	46607.9	4.89	66	44	50.46	60.77	-0.714

Table 3. Information about proteins interacting with UBR7-domino

Accession[a]	Description	Mass	Score	Matches[b]	Sequences[c]	emPAI	Coverage
gi|284810746	nucleocapsid protein [*Tomato spotted wilt orthotospovirus*]	29094	650	34(23)	16(12)	4.08	51%
gi|729042213	glyceraldehyde 3-phosphate dehydrogenase-A [*Nicotiana benthamiana*]	42945	115	10(5)	7(5)	0.45	19%
gi|926663240	heat shock protein 90-1 [*Nicotiana benthamiana*]	80443	94	6(3)	5(2)	0.08	6%
gi|1219878403	Gc-Gn glycoprotein precursor [*Chrysanthemum stem necrosis orthotospovirus*]	130189	89	6(4)	5(4)	0.10	4%
gi|660450867	domains rearranged methyltransferase 1 [*Nicotiana benthamiana*]	69106	78	4(4)	1(1)	0.05	0%

[a] the protein number in NCBI.

[b] the total number of peptides matched, in brackets is the number of matches higher than the significance threshold.

[c] the total number of sequences matched, in brackets is higher than the significance threshold sequence number.

Figures

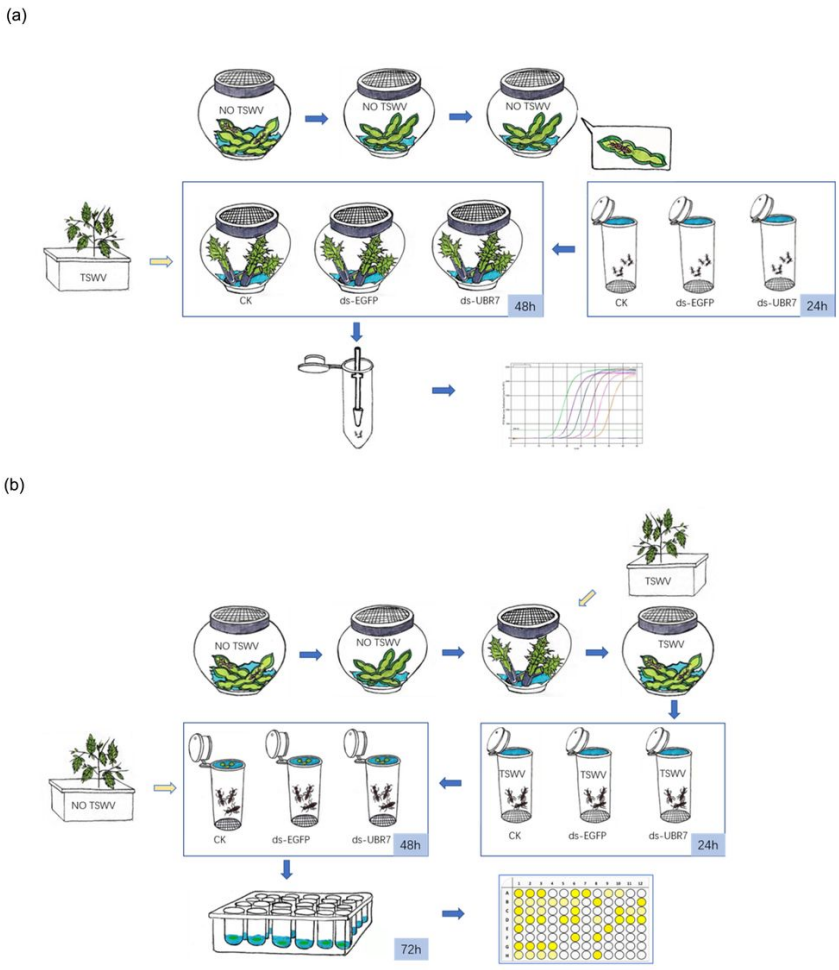

Figure 1

Procedure of RNA interference experiments in *Frankliniella occidentalis*

(a) Experiments on acquiring TSWV of *F. occidentalis*. Collected L1s were divided into three groups (CK, ds-EGFP, and ds-UBR7) and were fed an artificial diet for an AAP. After 24 h, thrips were fed *D. stramonium* plants with TSWV. After 48 h, the leaves were replaced with healthy beans until thrips reached the L2s. The TSWV abundance of L2 thrips was detected using qPCR.

(b) Experiments on acquiring TSWV of *F. occidentalis*. Collected L1s were allowed to feed on TSWV-infected *D. stramonium* leaf tissue for an AAP of 72 h. Then, thrips were transferred to cups with green beans until 3 days after emergence. Adults with TSWV (V+) were divided into three groups (CK, ds-EGFP, and ds-UBR7) and were allowed to feed an artificial diet for an AAP. After 24 h, the artificial diet was replaced with the true leaf of a healthy *D. stramonium*, a small disc with a diameter of 5 mm. Three small disks were placed in each small cage. After 48 h, small disks were removed and placed in a 24-well plate, 1 mL ddH_2O was added to each well, and the plate were placed in a light incubator for 72 h. Then, ELISA was used to detect the poisoning rate of leaves.

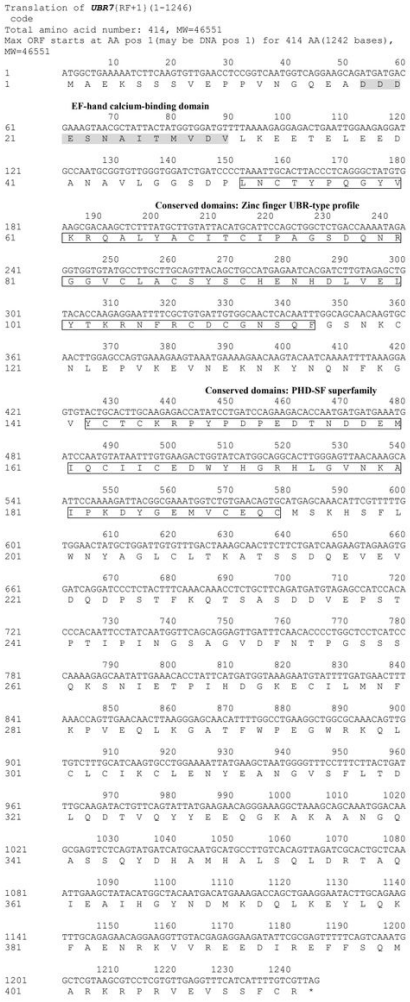

Figure 2

Nucleotide and deduced amino acid sequence of the *UBR7* cDNA in *Frankliniella occidentalis*.

The sites of the conserved motifs are marked with a box. The EF-hand calcium-binding domain is shaded. The asterisk indicates the termination codon.

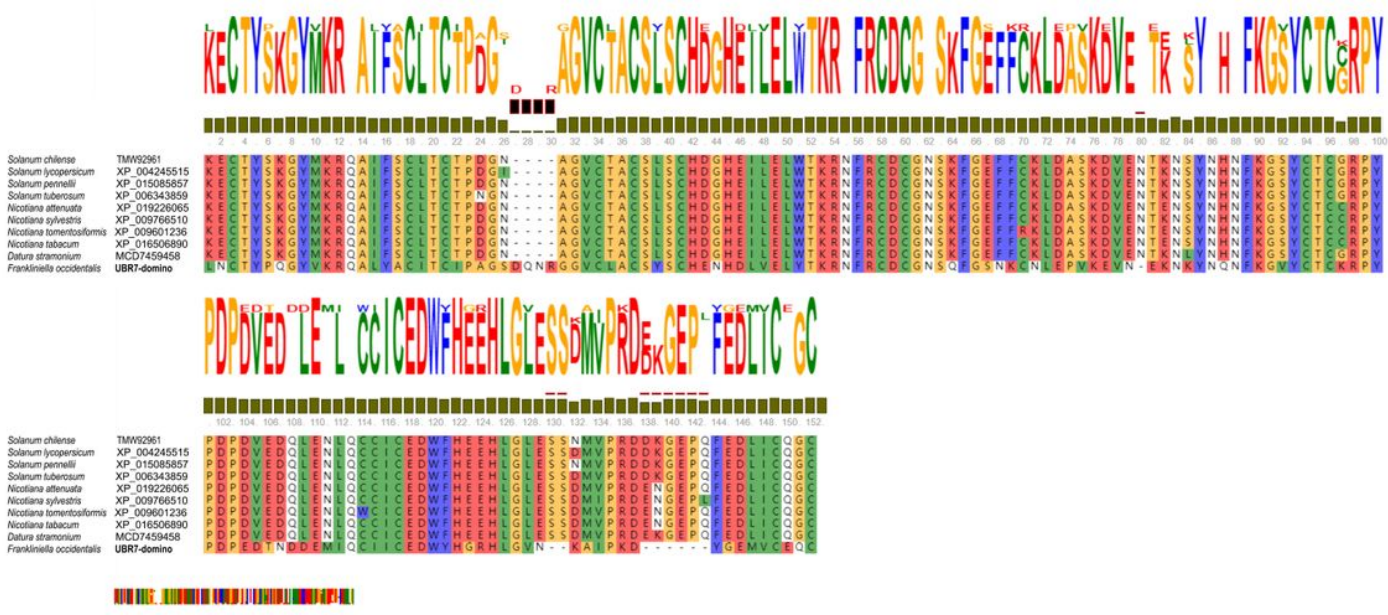

Figure 3

Multiple sequence alignment of *Frankliniella occidentalis* UBR7-domino amino acid sequences with Solanaceae plants.

Conserved amino acid residues are indicated by the same background color. Gaps (–) were introduced into the sequences to optimize alignment. Little black squares: gene absence/presence variations. Little brown square: conservation weights.

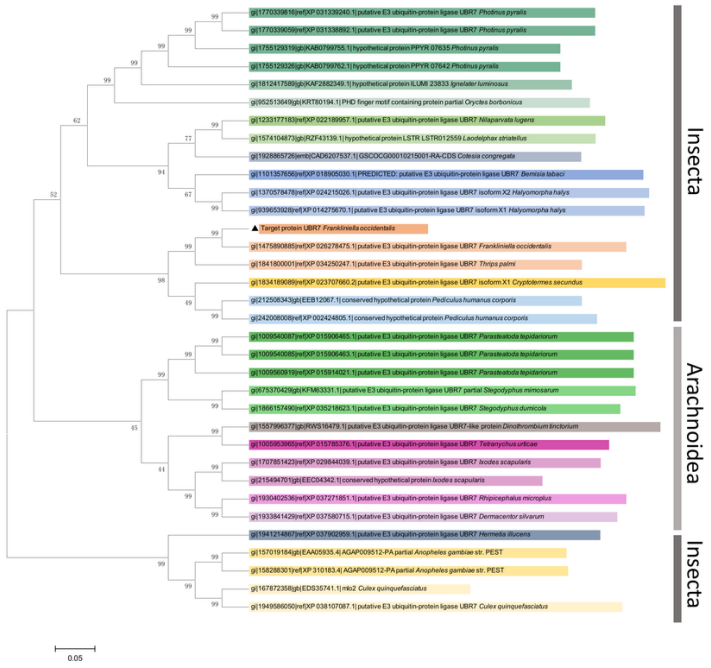

Figure 4

Phylogenetic analysis of *UBR7* gene sequences in *Frankliniella occidentalis*.

The maximum likelihood tree illustrates the phylogenetic relationship of *UBR7* in *F. occidentalis* with other arthropod E3 ubiquitin–protein ligases. The neighbor-joining method generated the phylogenetic tree with 1000 bootstrap replicates using MEGA 5.0 according to the AAs. The numbers above the branches support the phylogenies from AAs, and only values above 40% are shown. The tree is drawn to scale, wherein branch lengths are in the same units as those of the evolutionary distances used to infer the phylogenetic tree.

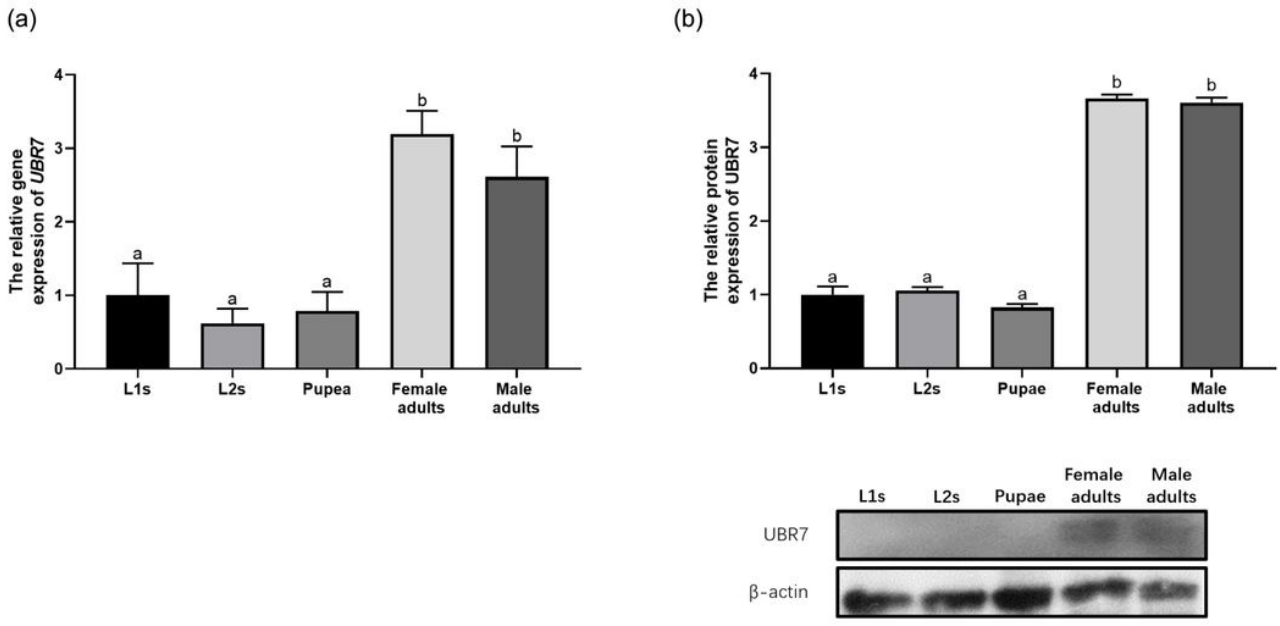

Figure 5

Expression of *UBR7* gene in *Frankliniella occidentalis.*

(a) The relative gene expression of *UBR7* in different instars (L1s, L2s, pupae, female adults, and male adults) of *F. occidentalis* (V^{-}). (b) Western blot was performed to detect the expression levels of UBR7. β-Actin was used as the loading control.

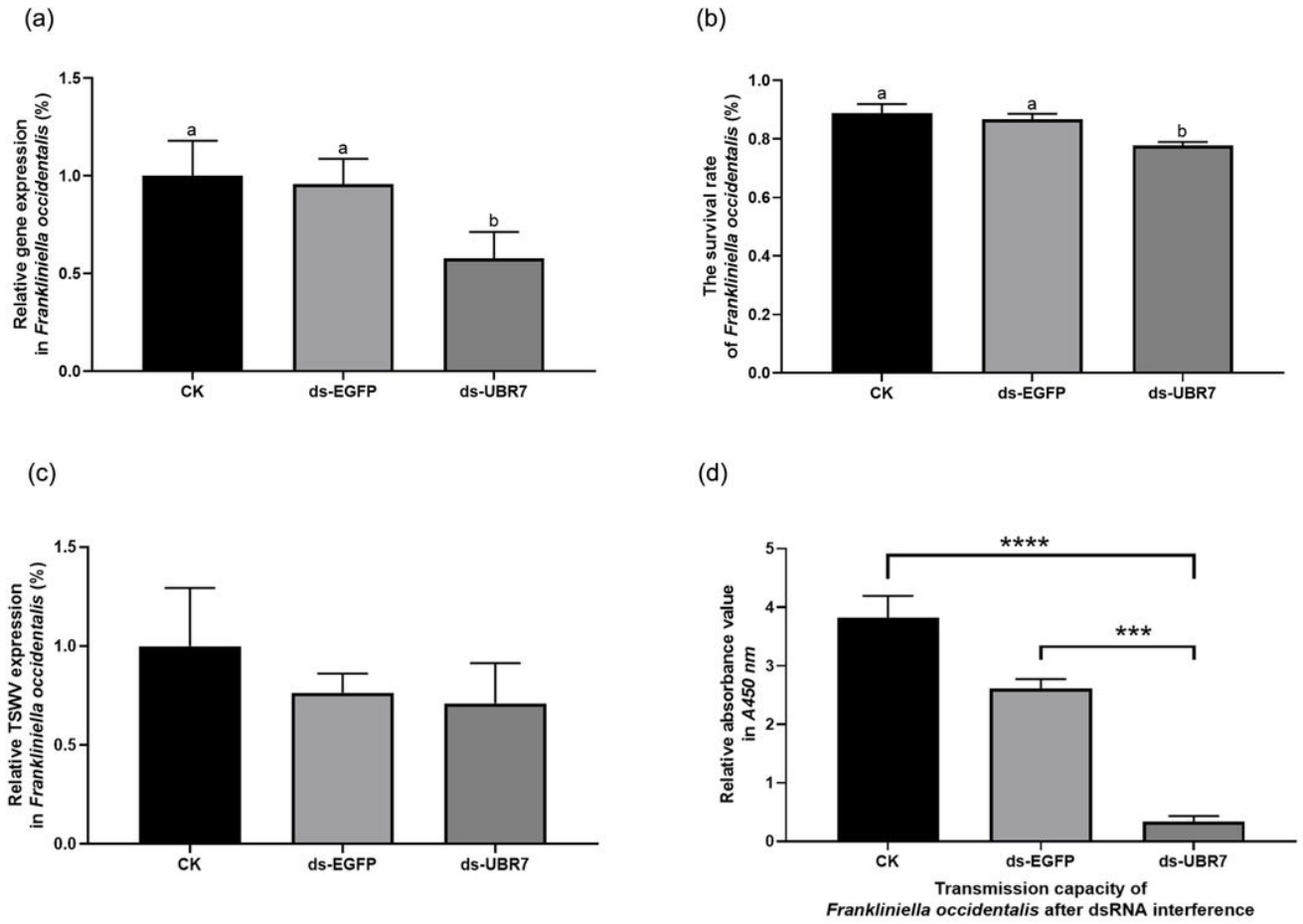

Figure 6

Effects of *UBR7* RNA interference on *Frankliniella occidentalis*.

(a) The relative gene expression of *UBR7* in *F. occidentalis* (V^-) after RNAi was detected using qPCR. Actin was used as the reference gene. (b) After RNAi, the survival rate of *F. occidentalis* (V^-) was counted (survival rate = the number of live thrips after interference/the number of live thrips before interference). (c) The operating procedure of the experiment on the effect of RNA interference on the ability of *F. occidentalis* to acquire TSWV. (d) After RNAi, the ability of *F. occidentalis* to acquire TSWV using qPCR to detect the abundance of TSWV in *F. occidentalis* (V^-). Actin was used as the reference gene. (e) The operating procedure of the experiment on the effect of RNA interference on the ability of *F. occidentalis* to spread TSWV. (f) After RNAi, DAS-ELISA was used to detect the transmission efficiency of *F. occidentalis* (V^+).

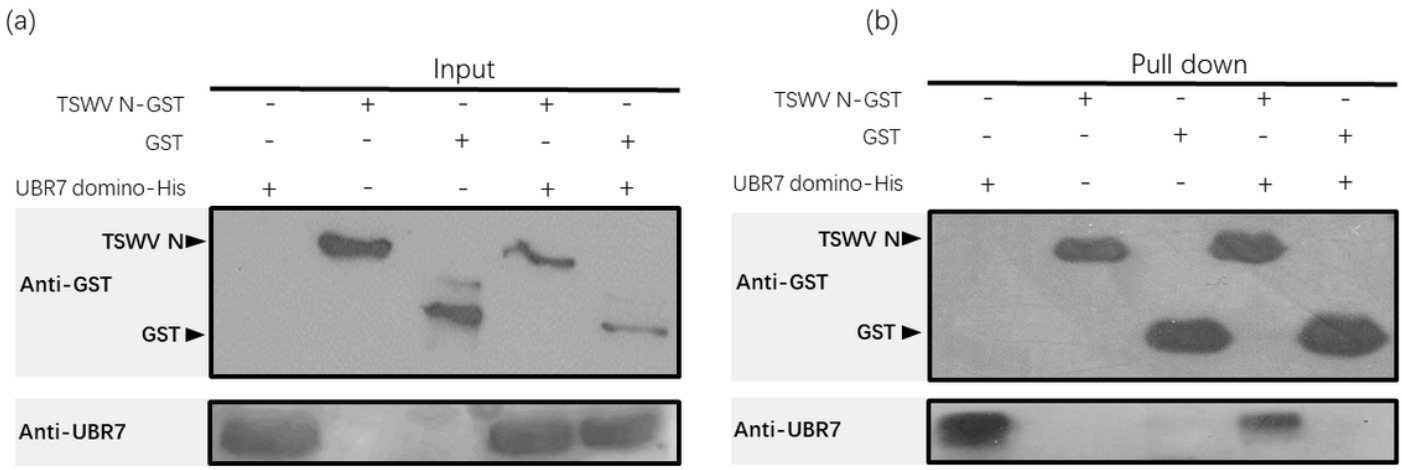

Figure 7

UBR7 protein in *Frankliniella occidentalis* interacts directly with the nucleocapsid protein of TSWV.

The GST pull-down assay examined the interaction between UBR7 and TSWV N.

Anti-GST and anti-UBR7 antibodies were used to test input and pull-down samples. (a) Input proteins before the GST-bead pull down. (b) Pull-down proteins after the GST-bead pull down.